

Adsorption-driven tuning of the electrical resistance of nanoporous gold

Patrick Wahl, Thomas Traußnig, Stephan Landgraf, Hai-Jun Jin, Jörg Weissmüller, and Roland Würschum

Citation: *Journal of Applied Physics* **108**, 073706 (2010); doi: 10.1063/1.3490789

View online: <http://dx.doi.org/10.1063/1.3490789>

View Table of Contents: <http://scitation.aip.org/content/aip/journal/jap/108/7?ver=pdfcov>

Published by the AIP Publishing

Articles you may be interested in

[Electrostatic correlations on the ionic selectivity of cylindrical membrane nanopores](#)

J. Chem. Phys. **140**, 064701 (2014); 10.1063/1.4864323

[Sign-inversion of charging-induced variation of electrical resistance of nanoporous platinum](#)

J. Appl. Phys. **112**, 073703 (2012); 10.1063/1.4755808

[Adsorption-driven translocation of polymer chain into nanopores](#)

J. Chem. Phys. **136**, 214901 (2012); 10.1063/1.4720505

[Electric field induced reversible tuning of resistance of thin gold films](#)

J. Appl. Phys. **104**, 103707 (2008); 10.1063/1.3020526

[N H 3 adsorption and decomposition on Ir\(110\): A combined temperature programmed desorption and high resolution fast x-ray photoelectron spectroscopy study](#)

J. Chem. Phys. **122**, 184705 (2005); 10.1063/1.1893690

**SHIMADZU**
Excellence in Science

Powerful, Multi-functional UV-Vis-NIR and FTIR Spectrophotometers

Providing the utmost in sensitivity, accuracy and resolution for applications in materials characterization and nano research

- Photovoltaics
- Polymers
- Thin films
- Paints
- Ceramics
- DNA film structures
- Coatings
- Packaging materials

[Click here to learn more](#)

Four Shimadzu spectrophotometers are shown. From left to right: a small benchtop model, a larger benchtop model with a sample holder, a large floor-standing model with a sample holder, and a large floor-standing model with a sample holder and a control panel.

Adsorption-driven tuning of the electrical resistance of nanoporous gold

Patrick Wahl,¹ Thomas Traußnig,¹ Stephan Landgraf,² Hai-Jun Jin,³ Jörg Weissmüller,^{3,a)} and Roland Würschum^{1,b)}

¹*Institute of Materials Physics, Graz University of Technology, Petersgasse 16, A-8010 Graz, Austria*

²*Institute of Physical and Theoretical Chemistry, Graz University of Technology, Technikerstr. 4, A-8010 Graz, Austria*

³*Institute of Nanotechnology, Karlsruhe Institute of Technology, D-76021 Karlsruhe, Germany*

(Received 2 June 2010; accepted 21 August 2010; published online 8 October 2010)

The electrical resistance of nanoporous gold prepared by dealloying is tuned by charging the surfaces of the porous structure in an electrolyte. Reversible variations in the resistance up to approximately 4% and 43% occur due to charging in the regimes of double layer charging and specific adsorption, respectively. Charging-induced variations in the electron density or of the volume cannot account for the resistance variation, indicating that this variation is primarily caused by charge-induced modifications of the charge carrier scattering at the solid-electrolyte interface. The relative resistance variation in nanoporous Au with surface charging is found to be much higher than reported for porous nanocrystalline Pt. This is due to the lesser resistance contribution from internal grain boundaries. The resistance variation in nanoporous Au is also higher than that found in thin films owing to the stronger surface scattering in the ligament structure compared to plan surfaces. We argue that the strong resistance variation in up to 43% in the regime of specific adsorption is due to the reversible formation of a chemisorbed surface layer acting as scattering centers for the charge carriers. © 2010 American Institute of Physics. [doi:10.1063/1.3490789]

I. INTRODUCTION

In the research field of metallic nanomaterials¹ the concept of property tuning by charging of interfaces has recently attracted interest in view of promising application potentials.^{2,3} Charge-induced or electrical field-induced tuning of materials properties is usually restricted to nonmetals such as semiconductors and piezoelectric ceramics. It could be shown recently that such a tuning can also be achieved with metals when the limits associated with the efficient electronic screening are overcome by a high number of interfaces, i.e., a high surface-to-volume ratio, as available in highly porous nanophase metals. Upon immersing this kind of porous metals in a liquid electrolyte, high surface charge densities can be achieved at the surface-electrolyte interface. In this way, charging-induced reversible variations in the lattice spacing and macroscopic length³ as well as of the magnetic susceptibility⁴ and electrical resistance⁵ of cluster-assembled porous nanocrystalline metals could be demonstrated.

A class of materials, which appears particularly attractive for charging of these kind, are nanoporous metals prepared by dealloying such as nanoporous (np)-Au.⁶ Compared to cluster-assembled nanocrystalline metals, effects associated with charging at surface-electrolyte interfaces are expected to be enhanced in nanoporous metals prepared by dealloying owing to the reduced influence of interfaces between the crystallites, i.e., grain boundaries. Both charge-induced^{7,8} and surface-chemistry driven actuation (i.e., length change)⁹ could be observed in np-Au.

Based on recent studies of the tunable electrical resistance of nanocrystalline metals by our group⁵ and others,¹⁰ the present work aims at studies of the resistance variation in nanoporous Au upon charging. Compared to recent measurements of this kind by Mishra *et al.*,¹¹ charging in the present work is extended to the regime of chemisorption by means of which resistance variation in np-Au larger than 40% can be realized. The present results on the charge-induced tuning of the resistance of nanoporous Au are compared with corresponding studies on thin films.¹²

II. EXPERIMENTAL PROCEDURE

The master alloy Ag₇₅Au₂₅ (at. %) was prepared from high purity Au and Ag ingot material (wires of purity 99.9%) by arc-melting and subsequent homogenization at 950 °C for more than 70 h (see Ref. 8). Thin foils were obtained by rolling to a thickness of ~100 μm. Between the rolling steps and afterwards, the samples were annealed several times at 600 °C for 2 h. For dealloying stripes with dimensions of ~20 × 5 × 0.1 mm³ were cut. Different dealloying procedures were applied in order to prepare nanoporous Au without oxygen adsorption layer (sample set I denoted “pure” in the following) and with an initial oxygen adsorption layer (sample set II, denoted “oxygen adsorbed” in the following).

Sample set I of pure nanoporous Au was prepared by dealloying the Ag₇₅Au₂₅ master alloy in diluted HNO₃ (volume ratio: 1:2) under potentiostatic control versus Ag/AgCl reference electrode. In order to avoid precipitation of Ag during dealloying, 1 M KNO₃ was used as salt bridge between the HNO₃ electrolyte and the 1 M KCl reference electrode. A tungsten rod (diameter 1 mm) was used as the counter electrode. The dealloying was performed at a voltage

^{a)}Present address: Hamburg University of Technology, Institute of Materials Physics and Technology, D-21073 Hamburg, Germany.

^{b)}Electronic mail: wuerschum@tugraz.at.

of +1.30 V versus Ag/AgCl and stopped after approximately 5 h when the current fell below a threshold of 1 mA. After the dealloying process the sample was removed and rinsed with distilled water. The samples for set II (oxygen adsorbed sample) were dealloyed in 1 M HClO₄ solution at a constant potential of +0.75 V (versus Ag/AgCl in 1 M HClO₄) as described previously.⁸ After dealloying, a higher potential (+0.85 V) was applied for a few hours to further stabilize the structure size. The ligament size of the nanoporous Au samples is in the range of 20 nm.⁸

The resistance measurements were performed in a standard electrochemical cell at ambient temperature using a potentiostat PGZ-100 (Votalab Comp.) for charging with the specimen being immersed in an aqueous electrolyte solution of 1 M KOH. The nanoporous Au specimen for resistance measurements served as working electrode. A commercial Pt-electrode (Radiometer Analytical) was used as counter electrode and a Ag/AgCl electrode (saturated KCl; Radiometer Analytical) as reference electrode. The dc electrical resistance was measured *in situ* in the cell by means of the four point method using a high-precision source and multimeter Type 2400 (Keithley Comp.). For contacting the np-Au sample, soft springs made of Au wires (diameter 0.25 mm, Chempur, purity 99.9%) were used, four electrodes for the resistance measurement and one for charging.

Charging of the pure np-Au sample (I) was performed by multistep chronoamperometric measurements. The voltage applied to the work electrode was incremented in steps of 100 mV at intervals of 2 min in the double layer regime and 3–30 min in the chemisorption regime. For each step, the charge quantity was determined by integrating the charging current making a correction for the leak current of 40 μ A in the double layer regime and up to 250 μ A in the chemisorption regime. In order to minimize errors due to this leak current, which may arise from Faraday current, the electrical resistance was recorded with a measuring current of 100 mA. Data points of the resistance were taken at the end of each charging interval when a constant value was attained. By reversing the sign of the measuring current it was further checked that the charging current did not affect the resistance measurement. Prior to the measuring run, cyclic voltammograms with scan rates of 1 mV/s were recorded in order to choose the appropriate potential range for charging in the double layer regime or in the regime of specific adsorption.

The resistance of the np-Au sample with the initial oxygen adsorbate (II) was monitored concurrently during cyclic voltammetric scanning. In this case, the charge in dependence of charging voltage was determined separately by chronoamperometric measurements.

III. RESULTS

Results of electrical resistance measurements on pure nanoporous Au in dependence of voltage U_{charging} used for charging in the range -700 and $+100$ mV are shown in Fig. 1(a). The corresponding variation with the imposed specific surface charge ΔQ upon cycling is depicted in Fig. 1(b). A fully reversible variation in the electrical resistance of approximately 6% occurs, where adding or removing of elec-

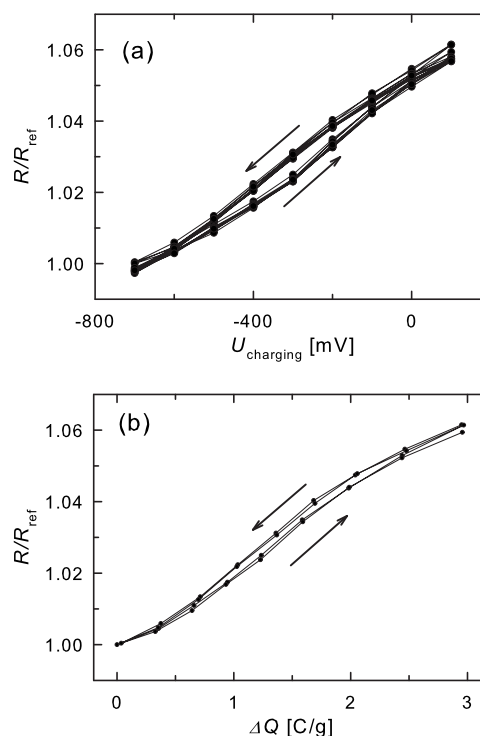


FIG. 1. Variation in resistance R of nanoporous Au (sample I) with (a) voltage U_{charging} used for charging and with (b) corresponding imposed charge ΔQ during consecutive chronoamperometric cycles between $U_{\text{charging}} = -700$ mV and $+100$ mV. ΔQ is obtained by integration the charging current; ΔQ and the reference value R_{ref} of the resistance refer to $U_{\text{charging}} = -700$ mV. The charge coefficient $(\Delta R/R)/\Delta Q$ given in Table I is obtained from the linear portion of the curve which corresponds to the double layer regime between -500 and -100 mV (see Fig. 2). U_{charging} measured with respect to Ag/AgCl reference electrode.

trons gives rise to a decrease or increase in R , respectively. The variation in R with U_{charging} [Fig. 1(a)] in this regime is nearly independent of the direction of charging, indicating that this variation is due the imposed surface charge (i.e., double layer formation) rather than due to chemical effects. This conclusion is further supported by cyclic voltammograms of the np-Au sample (Fig. 2). From the linear part $(\Delta R/R = 4\%)$ of the $\Delta R - \Delta Q$ curve [Fig. 1(b)] a charge coefficient $(\Delta R/R)/\Delta Q = 2.2 \times 10^{-2}$ g/C can be deduced (Table I).

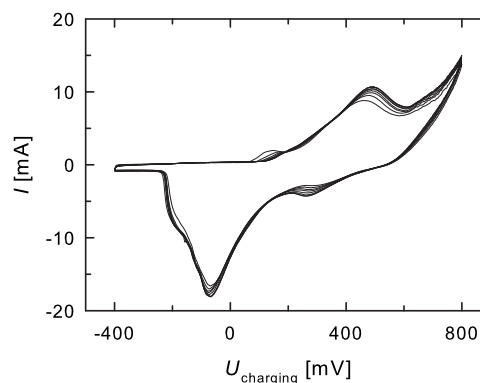


FIG. 2. Charging current I vs charging voltage U_{charging} during successive eight cycles at 1 mV/s of sample I (cyclic voltammogram). U_{charging} measured with respect to Ag/AgCl reference electrode. Peaks above $U_{\text{charging}} = +100$ mV (anodic direction) and at $U_{\text{charging}} = -100$ mV (cathodic direction) indicate specific adsorption of oxygen species and desorption, respectively. Double layer regime between -500 and -100 mV.

TABLE I. Maximum relative variation $(\Delta R/R)_{\max}$ and charge coefficient $(\Delta R/R)/\Delta Q$ of the relative resistance variation in np-Au with charging (sample I and II). ΔQ : charge density related to mass (C/g) or surface area (C/m²) (quoted in brackets). The different charging regimes A, B, and C of sample II are shown in Fig. 4. Literature values for np-Au, cluster-assembled porous nanocrystalline Pt (nc), and thin Au films are shown for comparison.

	$(\Delta R/R)_{\max}$	$(\Delta R/R)/\Delta Q$ (10 ⁻² g/C) [(10 ⁻² m ² /C)]	Charging regime	Remarks
np-Au, I	0.04	2.2	Double layer	Fig. 1
	0.43	0.9	Specific adsorption	Fig. 3
np-Au, II		1.4	(A) initial, with oxide	Fig. 4
		2.0	(B) double layer	Fig. 4
	0.19	0.6	(C) specific adsorption	Fig. 4
np-Au ^a	0.06	3.3	Double layer	
nc-Pt ^b	0.08	0.3	Double layer	
Au, thin film (7 nm) ^c	0.016	0.7 (5.3)	Double layer	
Au, thin film (25 nm) ^d	0.15	1.0 (2)	Specific adsorption	

^aReference 11.

^bReference 5.

^cReference 19.

^dReference 21.

Upon increasing the charging voltage toward more positive values, the regime is reached ($U_{\text{charging}} > 100$ mV) where specific adsorption of negative ions occurs as shown in the cyclic voltammogram in Fig. 2. The most common interpretation is the chemisorption of oxygen atoms to the Au surface (Au–OH and Au–O). This electrochemical process is reversed upon charging in the cathodic direction which gives rise to desorption with a maximum at $U_{\text{charging}} = -100$ mV. Cycling in this extended voltage range of specific adsorption and desorption gives rise to a pronounced increase in the charge-induced resistance variation as compared to the regime of double layer charging. The resistance increases reversibly by approximately 43% upon cycling between -400 and $+800$ mV. The R - U_{charging} characteristic shows a significant hysteresis [Fig. 3(a)]. The much larger resistance variation in the regime of specific adsorption and desorption as compared to the double layer is due to the higher charge imposed chemically [compare ΔQ in Figs. 3(b) and 1(b)]. Although the resistance variation in the chemical regime is much higher, the charge coefficient $(\Delta R/R)/\Delta Q$ is

more than $2\times$ smaller compared to the double layer regime (Table I).

The charging-induced resistance variation in the np-Au sample (II) with the initial adsorbed oxygen layer is shown in Fig. 4. Upon cycling in the positive voltage regime (A, Fig. 4), where the initial adsorbed oxygen layer is stable,⁸ the resistance changes reversibly between a lower value at $U_{\text{charging}} = +300$ mV and a higher value at $U_{\text{charging}} = +600$ mV corresponding to a charge coefficient $(\Delta R/R)/\Delta Q = 1.4 \times 10^{-2}$ g/C. Removing the oxygen layer by a cathodic sweep from $U_{\text{charging}} = +300$ mV to -400 mV gives rise to an irreversible decrease in R by a factor of approximately 1.8. Subsequent cycling in the double layer regime (B, Fig. 4) is associated with a slightly larger resistance variation [$(\Delta R/R)/\Delta Q = 2.0 \times 10^{-2}$ g/C, Table I] as compared to the initial state. Extending the voltage regime from -400 mV/ $+100$ mV to -400 mV/ $+600$ mV into the chemical regime where specific adsorption and desorption of negative ions occurs, the resistance variation substantially increases ($\Delta R/R = 19\%$). Similar to the pure sample (I), how-

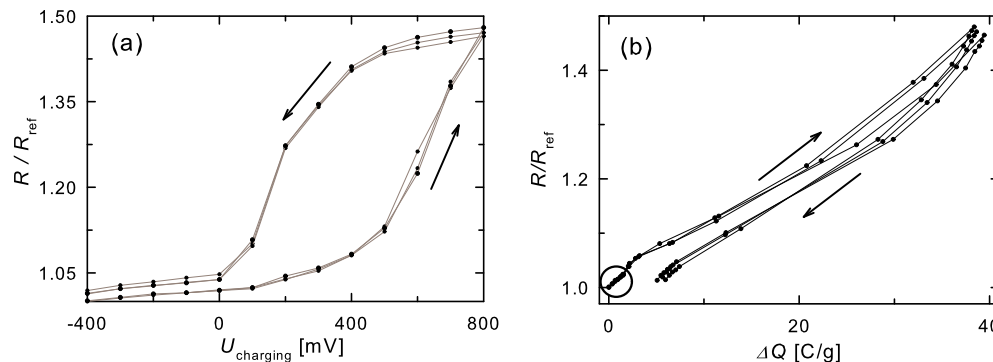


FIG. 3. (Color online) Variation in resistance R of nanoporous Au (sample I) with (a) voltage U_{charging} used for charging and with (b) corresponding imposed charge ΔQ during consecutive chronoamperometric cycles between $U_{\text{charging}} = -400$ mV and $+800$ mV which includes the regime of chemical adsorption and desorption (see Fig. 2). The encircled range in part (b) represents the double layer regime. ΔQ is obtained by integration of the charging current; ΔQ and the reference value R_{ref} of the resistance refer to $U_{\text{charging}} = -400$ mV. The charge coefficient $(\Delta R/R)/\Delta Q$ given in Table I is obtained from the entire regime between -400 and $+800$ mV. U_{charging} measured with respect to Ag/AgCl reference electrode.

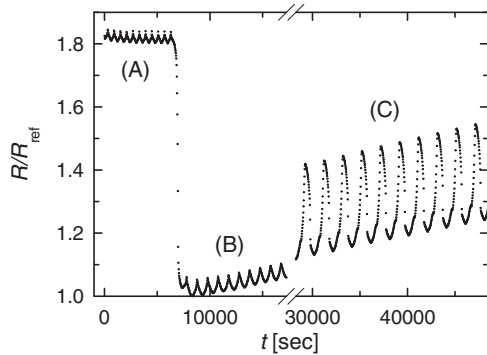


FIG. 4. Variation in resistance R of nanoporous Au (sample II) with time t upon reversible cycling between (a) $U_{\text{charging}} = +300$ and $+600$ mV, (b) -400 and $+100$ mV, and (c) -400 and $+600$ mV. The cycling regimes correspond to (a) the state with the initial as-prepared oxygen adsorbed layer and (b) the double layer or (c) chemical adsorption and desorption after irreversible removal of the initial adsorbed layer. The charge coefficients $(\Delta R/R)/\Delta Q$ of the three regimes are given in Table I. R_{ref} denotes the minimum resistance in the double layer regime. U_{charging} measured with respect to Ag/AgCl reference electrode.

ever, the charge coefficient $(\Delta R/R)/\Delta Q = 0.6 \times 10^{-2}$ g/C in the regime of specific adsorption and desorption is significantly smaller as compared to the double layer regime (Table I).

It is worthwhile to mention that upon removal of the oxygen layer, the resistance slightly drifts with time upon consecutive cycling (part B and C, Fig. 4) which may indicate some structural reordering on a longer time scale after desorption of oxygen. Prior to the removal of oxygen (part A, Fig. 4), no significant drift of the resistance occurs. The same pertains to sample I indicating that in those cases a quasistationary state without structural reordering prevails.

IV. DISCUSSION

The present measurements on nanoporous Au in dependence of charging in an electrolyte reveal as a major result that the resistance can be varied in the several percentage range or by up to 43% upon charging in the double layer or chemical regime, respectively. The charge coefficient $(\Delta R/R)/\Delta Q$ in double layer regime is $2.4\text{--}3.3 \times$ higher than in the regime of specific adsorption (Table I).

At first, the resistance variation in the double layer regime will be addressed. The presently observed charge-induced resistance change in the double layer regime fits quite well to that observed by Mishra *et al.*¹¹ recently on np-Au (compare charge coefficients in Table I). For discussion of the resistance variation, we start from the free electron model of conductivity¹³

$$\sigma = \frac{e^2 n \tau}{m}, \quad (1)$$

where e , m , n , and τ^{-1} denotes the electron charge, the electron mass, the charge carrier density and the scattering rate, respectively. Charging may affect the resistance in different ways, namely by variation in (i) the charge density, (ii) the volume, or (iii) the scattering rate. As we will see in the following, the observed resistance variation has mainly to be attributed to a change in the scattering probability.

- (i) From the maximum variation in the net charge of $\Delta Q = 1.7$ C/g due to double layer formation in the regime $U_{\text{charging}} = -500$ to -100 mV, a volume averaged charge variation in $\Delta n/n = 3.5 \times 10^{-4}$ is estimated taking into account the free charge carrier density $n = 5.9 \times 10^{28} \text{ m}^{-3}$ of bulk crystalline Au. This value $\Delta n/n$ is by two orders magnitude lower than $\Delta R/R$ and, therefore, by far cannot account for the present charge-induced effect. This notion also holds for the actual situation that the imposed excess charge, arising from double layer formation, is concentrated at the nanostructure-electrolyte interface rather than being uniformly distributed in the nanostructure. This follows by describing the interconnected porous network as a cylindrical nanostructure for which the cylindrical surface shell with a modified carrier density and the cylindrical core act as parallel conduction paths.
- (ii) Next, we will consider the influence of a charge-induced variation in the volume on the electrical conductivity. Charging experiments on nanoporous pure Au revealed a reversible expansion $\Delta l/l = 0.4 \times 10^{-4}$ upon positive charging up to $\Delta Q = 0.8$ C/g.⁸ Taking into account the bulk modulus $K = 173$ GPa and the pressure coefficient $(\Delta R/R)/p = -3 \times 10^{-6} \text{ bar}^{-1}$ of the resistance of Au,¹⁴ this charge-induced volume expansion corresponds to a relative increase $\Delta R/R$ of the resistance of 6×10^{-4} . Therefore, also the charge-induced volume change cannot account for the observed value $\Delta R/R$ which is two orders of magnitude larger. This negligible effect of the volume on the resistance is further supported by another comparison. Although the charged-induced volume changes in the regimes of double layer charging and specific adsorption/desorption are almost identical,¹⁵ the relative resistance variations with respect to imposed charge are quite different in these regimes (see $(\Delta R/R)/\Delta Q$, Table I).
- (iii) Since the charging effect on the charge carrier density and the volume obviously cannot account for the observed resistance variation, one has to conclude that the observed charging-induced variation in the resistance predominantly arises from variations in the scattering probability τ^{-1} with charging. In fact, charge carrier scattering at the crystal-electrolyte interfaces is the dominating factor of the electrical resistance of the nanoporous structure. This is the case because the ligament size of about 20 nm, i.e., the structural dimension of nanoporous Au is of similar size or even smaller than the mean free path of electrons. Indeed, the mean free path l of conduction electrons in crystalline Au at ambient temperature is in the range of 40 nm as derived from Eq. (1) with the conductivity $\sigma = 4.55 \times 10^5 (\Omega \text{ cm})^{-1}$, the charge carrier concentration $n = 5.9 \times 10^{28} \text{ m}^{-3}$, and the Fermi velocity $v_F = l/\tau = 1.39 \times 10^8 \text{ cm/s}$ of Au (data taken from Ref. 16). The interpretation of the present results in terms of changes in the electron scattering probability at the crystal-electrolyte interfaces is in line with that given

by Tucceri and Posadas¹⁷ for the charge-dependence of the resistance of Ag films. According to these authors positive charging of the surface gives rise to localized scattering centers at the metal surface due to screening effects which leads to an increase in the resistance. This notion of charge-dependent interface scattering is also supported by recent *ab initio* studies according to which an outward or inward relaxation of the top layer of the surface atoms of Au occurs in response to negative or positive charging the surface, respectively.¹⁸

The theoretically predicted charge-induced relaxation of the surface,¹⁸ on the other hand, raises the question whether a variation in the thickness with charging associated with this relaxation may affect the resistance. In fact, merely because of a charge-induced thickness increase or decrease, the probability of charge scattering at the crystal-electrolyte interface is expected to decrease or increase, respectively. However, this effect should scale with the ratio of the charge-induced relaxation and the structure size. For a charge-induced relaxation well below 0.1 nm (Ref. 18) and a structural size in the range of 20 nm this ratio is at least one order of magnitude smaller than the observed relative resistance variation and, therefore, cannot account for the observed resistance variation. This conclusion regarding the effect of relaxation is fully consistent with that of the pressure effect discussed in paragraph (ii).

The interpretation in terms of charge-dependent scattering at the crystal-electrolyte interfaces is further supported by comparing the present results with corresponding measurements on particle-assembled nanocrystalline metals and on thin films. The charge coefficient in the double layer regime of the nanoporous sample is up to more than $7\times$ larger than that in cluster-assembled porous nanocrystalline Pt (Ref. 5) (Table I). This shows that in particle-assembled nanocrystalline Pt the influence of charge-dependent scattering at electrolyte interface is reduced as compared to porous Au due to strong scattering at particle-particle grain boundary interfaces.⁵ On the other hand, the charge coefficient of np-Au is also up to $3\times$ larger than that in Au film with a thickness of 7 nm (Table I) (Ref. 19) and even much larger than that in Ag films.¹⁷ This indicates that the scattering at the electrolyte interface in the nanoporous sample is stronger than in thin films as expected because of the more complex ligament structure compared to a plane surface-electrolyte interface of a film. A more quantitative description of the electrical transport properties should take into account this complex morphology which for instance can be numerically simulated on the basis of finite element methods.²⁰

Finally, the resistance variation in nanoporous Au in the regime of specific adsorption will be discussed. Upon cycling in the voltage range where specific adsorption or desorption of negative ions occurs, reversible resistance variations between up to 19% and 43% were found in the various nanoporous Au samples (see Figs. 3 and 4 and Table I). This resistance variation in the chemical regime of the nanoporous samples is of similar size (19%) or even higher (43%) than that observed by Ganon *et al.*²¹ upon electrochemical

adsorption and desorption of oxygen in Au films with thickness of 25 nm (Table I). In the latter case, the resistance increase upon positive charging in the chemical regime is ascribed to the reversible processes of adsorption and chemisorption of oxygen species (OH^- , O^{2-}) with the formation of an Au-oxide layer.²¹ An increase in the resistance of thin films is also observed for chemisorption of other negative ions.¹⁷

The study of the chemical nature of the chemisorbed layer is beyond the scope of the present work. From the maximum transferred charge of 40 C/g in the chemical regime [Fig. 3(b)] a charge transfer of about two electrons per surface atom can roughly be estimated, assuming a mass-specific surface area of 10 m²/g of np-Au,⁸ which corresponds to the formation of about one monolayer of chemisorbed species. Similar as discussed for the double layer regime [see paragraph (i)], the reduced number of charge carriers associated with one nonconducting chemisorbed monolayer in relation to the total number of charge carriers cannot account for the resistance variations in the range of 19%–43%. This supports the notion developed earlier for thin films^{17,21} that the resistance in the chemical regime increases because the atoms of the chemisorbed layer act as scattering centers thus modifying the scattering rate $1/\tau$.^{17,21} The present result that the charge coefficient $(\Delta R/R)/\Delta Q$ in this chemical regime is lower than in the double layer regime (Table I) also qualitatively agrees with observations on thin films.¹⁷

In conclusion, the present studies showed that the resistance of nanoporous Au can be reversibly tuned by means of charging the surfaces of the porous structure in an electrolyte. Reversible variations in the resistance of up to 43% occur due to the formation of a chemisorbed surface layer. Charge-induced modifications of the charge carrier scattering at the solid-electrolyte interface is identified as the dominant effect which causes the resistance variations. The relative resistance variation in nanoporous Au is found to be more pronounced in comparison to both porous cluster-assembled metals and thin films.

ACKNOWLEDGMENTS

Financial support by the Austrian Science Fund (FWF) is appreciated (Project No. S10405-N16).

¹H. Gleiter, *Prog. Mater. Sci.* **33**, 223 (1989).

²H. Gleiter, J. Weissmüller, O. Wollersheim, and R. Würschum, *Acta Mater.* **49**, 737 (2001).

³J. Weissmüller, R. Viswanath, D. Kramer, P. Zimmer, R. Würschum, and H. Gleiter, *Science* **300**, 312 (2003).

⁴H. Drings, R. Viswanath, D. Kramer, C. Lemier, and J. Weissmüller, *Appl. Phys. Lett.* **88**, 253103 (2006).

⁵M. Sagmeister, U. Brossmann, S. Landgraf, and R. Würschum, *Phys. Rev. Lett.* **96**, 156601 (2006).

⁶J. Erlebacher, J. Aziz, A. Karma, N. Dimitrov, and K. Sieradzki, *Nature (London)* **410**, 450 (2001).

⁷D. Kramer, R. Viswanath, and J. Weissmüller, *Nano Lett.* **4**, 793 (2004).

⁸H. Jin, S. Parida, D. Kramer, and J. Weissmüller, *Surf. Sci.* **602**, 3588 (2008).

⁹J. Biener, A. Wittstock, L. Zepeda-Ruiz, M. Biener, V. Zielasek, D. Kramer, R. Viswanath, J. Weissmüller, M. Bäumer, and A. Hamza, *Nature Mater.* **8**, 47 (2009).

- ¹⁰C. Bansal, S. Sarkar, A. Mishra, T. Abraham, C. Lemier, and H. Hahn, *Scr. Mater.* **56**, 705 (2007).
- ¹¹A. Mishra, C. Bansal, and H. Hahn, *J. Appl. Phys.* **103**, 094308 (2008).
- ¹²R. Tucceri, *Surf. Sci. Rep.* **56**, 85 (2004).
- ¹³J. Ziman, *Principles of the Theory of Solids* (Cambridge University Press, Cambridge, 1972).
- ¹⁴J. Bass, J. Dugdale, C. Foiles, and A. Myers, in *Numerical Data and Functional Relationships in Science and Technology*, Landolt-Börnstein, New Series, Group III, Vol. 15B, edited by K.-H. Hellwege and J. Olsen (Springer, Berlin, 1985), p. 435.
- ¹⁵H. Jin and J. Weissmüller, (unpublished).
- ¹⁶C. Kittel, *Introduction to Solid State Physics* (Wiley, New York, 1976).
- ¹⁷R. Tucceri and D. Posadas, *J. Electroanal. Chem.* **283**, 159 (1990).
- ¹⁸Y. Umeno, C. Elsässer, B. Meyer, P. Gumbsch, and J. Weissmüller, *EPL* **84**, 13002 (2008).
- ¹⁹S. Dasgupta, R. Kruk, D. Ebke, A. Hütten, C. Bansal, and H. Hahn, *J. Appl. Phys.* **104**, 103707 (2008).
- ²⁰C. Eilks and C. Elliot, *J. Comput. Phys.* **227**, 9727 (2008).
- ²¹J.-P. Ganon, C. Nguyen, and J. Clavilier, *Surf. Sci.* **79**, 245 (1979).